

Interplanetary drivers of ionospheric prompt penetration electric fields

Jianpeng Guo^{a,*}, Xueshang Feng^a, Pingbing Zuo^a, Jie Zhang^b, Yong Wei^c, Qiugang Zong^c

^a State Key Laboratory of Space Weather (Center for Space Science and Applied Research, Chinese Academy of Sciences), Beijing 100190, China

^b Department of Computational and Data Sciences, George Mason University, 4400 University Drive, MSN 6A2, Fairfax, VA 22030, USA

^c School of Earth and Space Sciences, Peking University, Beijing 100871, China

ARTICLE INFO

Article history:

Accepted 31 January 2010

Available online 10 February 2010

Keywords:

Interplanetary electric field

Equatorial electric field

MC structures

Electric field penetration

ABSTRACT

In this paper we discussed the penetration effects of common interplanetary magnetic cloud (MC) structures like sheath region, both sheath and magnetic cloud boundary layer (MCBL), MC body, and shock-running into a preceding MC on the equatorial ionosphere during intense ($SYM-H \leq -100$ nT) geomagnetic storms. Using solar wind data obtained from the ACE and WIND spacecraft, we have identified these four types of MC structures responsible for the electric field penetration events detected by Jicamarca incoherent scatter radar. After elimination of the propagation delay, the observations show that the equatorial electric field (EEF) was changed immediately following the arrival of solar wind disturbance. Moreover, the duration of EEF corresponded well with that of the corresponding MC structure interval. We suggest that identifying the solar wind structures associated with penetration electric field may shed light on the understanding of the penetration processes and further help exploring their effects on the ionospheric plasma.

© 2010 Elsevier Ltd. All rights reserved.

1. Introduction

Manifestations of coronal mass ejections (CMEs) originated from the Sun are frequently observed in the solar wind near the Earth and are commonly called interplanetary coronal mass ejections (ICMEs). A subset of ICMEs, called magnetic clouds (MCs), are defined as the structures having a smooth magnetic field rotation (interpreted as a morphology of magnetic flux rope) and enhanced magnetic field magnitude coupled with a reduced proton temperature and plasma beta (Burlaga et al., 1981). MC itself consists of the following two principal regions that both can drive strong magnetospheric activity (e.g., Tsurutani et al., 1988; Huttunen and Koskinen, 2004; Huttunen et al., 2008): (1) MC body consisting of the plasma and magnetic field from the CME eruption and (2) sheath of compressed and heated solar wind plasma ahead of the MC body. The sheath regions are often characterized by enhanced, fluctuating field strength, speed, density, and dynamic pressure. It is interesting to separate magnetospheric activity due to sheath and MC body since the solar wind parameters that control solar wind-magnetospheric coupling have a significantly different behavior during these structures. Within a sheath the dynamic pressure is typically high and variable and the magnetic field direction can change several

times from south to north while during the MC body the magnetic field direction typically changes smoothly over timescales of a day. In addition to sheath and MC body, front and tail “boundary layers” can be separated in an MC. Wei et al. (2003a) defined the boundary layer as a disturbance structure located between the MC body and the ambient solar wind. The MCBLs are characterized by the obvious magnetic signatures including the magnetic decrease inside the boundary layer like magnetic holes, the magnetic field azimuthal angle and the latitudinal angle change near the center of MCBLs, as well as the corresponding plasma features (relatively high proton temperature, high plasma beta, high proton density, and as a result high dynamic pressure) (Wei et al., 2003a; 2003b; 2006). Zuo et al. (2007) pointed out that the magnetic field Z component (B_z) has more turbulent structure inside boundary layers than inside sheath regions and MC body making boundary layers good candidates for triggering substorms. In addition, complex solar wind structures involving multiple MCs can be produced when two and more CMEs interact with each other in the interplanetary space (Burlaga et al., 2002; Gopalswamy et al., 2001).

Interplanetary electric fields, caused by the convection motion of the solar wind across the interplanetary magnetic field as inferred from $E = -V \times B$ (Tsurutani et al., 2008), may appear almost immediately in the Earth’s magnetosphere and ionosphere after these electric fields are convected from the solar wind to the magnetosphere. This phenomenon is commonly termed as the prompt penetration of the interplanetary electric field (IEF) into the magnetosphere/ionosphere system, or simply electric field penetration. Considerable efforts have been made to understand

* Corresponding author. Tel.: +86 10 6258 6354.

E-mail addresses: jpguo@spaceweather.ac.cn (J. Guo), fengx@spaceweather.ac.cn (X. Feng), pbzuo@spaceweather.ac.cn (P. Zuo), jzhang7@gmu.edu (J. Zhang), weiy@pku.edu.cn (Y. Wei), qgzong@gmail.com (Q. Zong).

how the IEF can penetrate into the low-latitude ionosphere (Nopper and Carovillano, 1978; Kikuchi and Araki, 1979; Kelley et al., 1979; Wolf et al., 2007). It is generally believed that a negative (southward) value of the north–south component of interplanetary magnetic field (IMF), B_z , can produce the efficient penetration of the electric fields, thanks to the occurrence of magnetic reconnection between the geomagnetic field and the IMF (Dungey, 1961). However, there were also reports showing the appearance of prompt penetration when IMF B_z is northward (e.g., Tsurutani et al., 2008). Manoj et al. (2008) studied the statistical characteristics of electric field penetration and found that the penetration of electric fields into the equatorial ionosphere has no significant dependence on the direction of IMF B_z . It had been suggested that the penetration electric fields could last only ~ 30 min because of a shielding effect by the ring current system (Senior and Blanc, 1984; Fejer et al., 1990). Huang et al. (2005) recently found that penetration electric fields can exist for a longer time and play a more significant role in the generation of ionospheric disturbances than what was previously thought. The penetration electric fields are detected in the magnetosphere and at the equatorial ionosphere with intensities of ~ 5 to 15% of the interplanetary electric field intensities (Kelley et al., 2003; Huang et al., 2007; Wei et al., 2008).

Recently, Nicolls et al. (2007) investigated the spectral properties of low latitude daytime electric fields and found that the integrated power in the equatorial electric field could increase by a factor of 100 as Kp increases from 0 to 8. Such evidence suggests that a significant part of the variability of the equatorial electric field is of interplanetary origin, as suggested by Earle and Kelley (1987). However, the structures of the interplanetary drivers of penetration electric fields have not been studied systematically to date. In this study, our focus is to discuss the penetration effects of common MC structures noted above on the equatorial ionosphere during intense ($\text{SYM-H} \leq -100$ nT) geomagnetic storms.

Using solar wind data obtained from the ACE and WIND spacecraft, we have identified four types of MC structures: sheath region, both sheath and magnetic cloud boundary layer (MCBL), magnetic cloud (MC) body, and shock-running into a preceding MC responsible for the electric field penetration events detected by Jicamarca incoherent scatter radar. The identification of the MC structures is based on a variety of signatures in the solar wind plasma and magnetic field, including plasma composition/charge state data from the SWICS instrument on ACE (Zurbuchen and Richardson (2006) and references therein). We also refer to an updated version of the “comprehensive” ICME list compiled by Cane and Richardson (2003) that also considers additional ICME

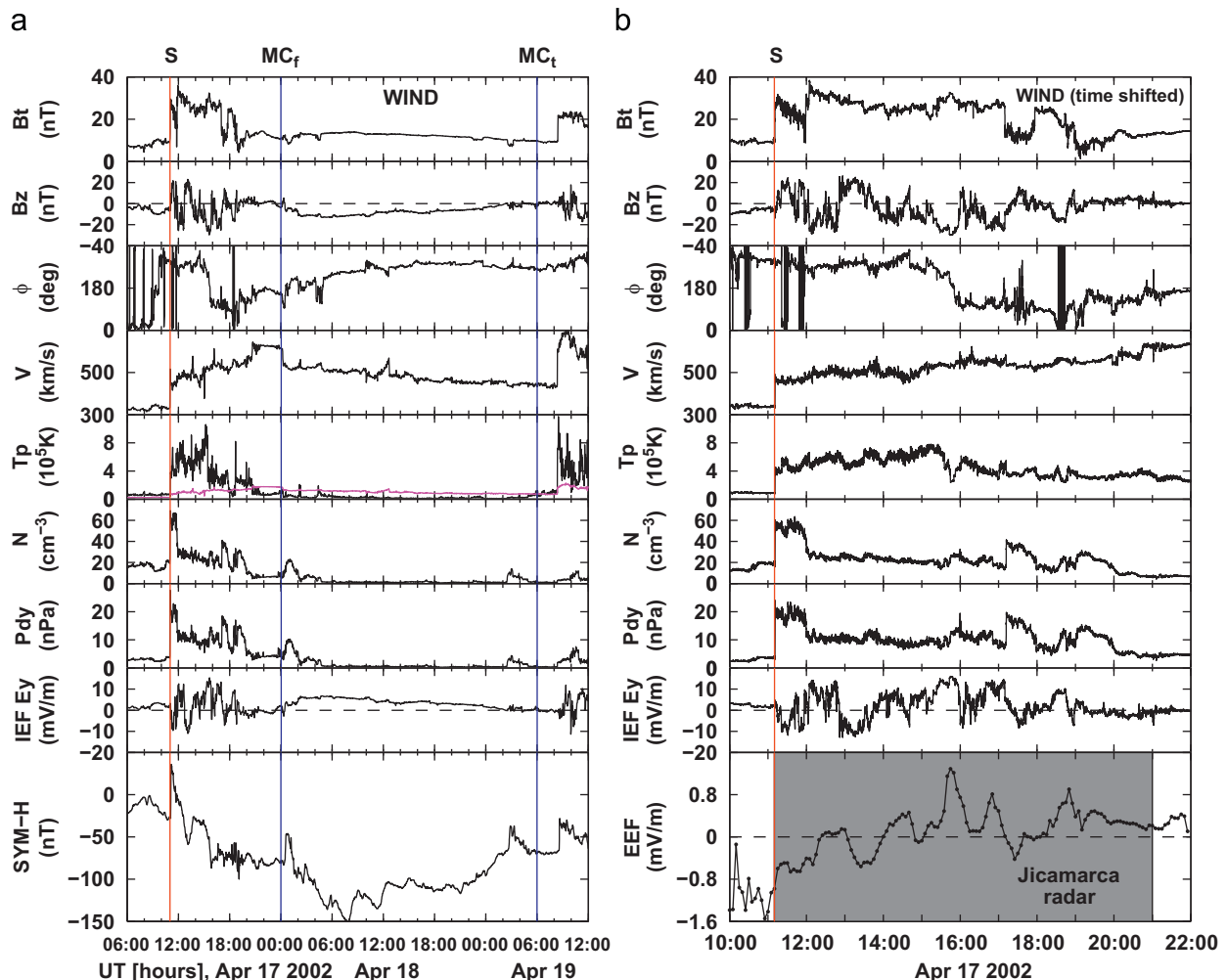


Fig. 1. (a) Interplanetary parameters and geomagnetic SYM-H index during 17–19 April 2002. The solar wind data are from WIND in GSM coordinates and include the magnetic field intensity, the B_z component, the magnetic field azimuth, the solar wind velocity, the proton temperature overlaid with the expected temperature (thick solid) (Richardson and Cane, 1995), the solar wind density, the solar wind dynamic pressure and the Y component of the electric field. The three vertical lines (S, MC_f and MC_t) from left to right indicate the shock arrival time, MC starting time, and MC ending time, respectively. (b) The equatorial electric field (EEF) measured by the Jicamarca radar on 17 April 2002 and the corresponding solar wind data (time shift of solar wind propagation time to magnetopause is applied). The shaded interval denotes the occurrence of the penetration electric field. The same format is used for Figs. 2–4.

signatures, in particular solar wind ion composition and charge state anomalies (Lepri et al., 2001; Richardson and Cane, 2004). The updated list is available at <http://www.ssg.sr.unh.edu/mag/ace/ACELists/ICMetable.html>. The identification of the IEF penetration is based on the phenomenon that reorientations of IMF can cause prompt changes in the EEF. The following section illustrates these types of solar wind structures that gave rise to ionospheric prompt penetration electric fields during intense geomagnetic storms. Section 3 is reserved for summary and discussion.

2. Observations

We used solar wind plasma and magnetic field measurements from the SWE, 3DP and MFI instruments on the WIND satellite and the SWEPAM and MAG instruments on board the ACE satellite (in GSM coordinates). These measurements were also used to calculate the solar wind dynamic pressure ($P_{dy} = N m_p V^2$) and the Y component of the interplanetary electric field (IEF E_Y ; $E_Y = V_x B_z$), where N , m_p and V are solar wind number density, proton mass, and solar wind speed, respectively. Note that the data from WIND and ACE were time compensated to a common point by interpolating the data point using the nearest neighbor interpolation methods. The symmetric current index SYM-H was used as an indicator of the level of geomagnetic activity. Equatorial zonal electric fields were obtained from vertical plasma drift

observations by the incoherent scatter radar at Jicamarca (11.92 °S, 76.87 °W, Dip latitude 1 °N). The radar data are recorded in 5 min sampling interval. The ionospheric electric field data are averaged over the altitude range of 248–368 km or determined from the Doppler shifts of 150-km echoes (Chau and Woodman, 2004). Examples of penetration events associated with four types of MC structures: sheath region, both sheath and magnetic cloud boundary layer (MCBL), magnetic cloud (MC) body, and shock-running into a preceding MC are shown in Figs. 1–4, respectively.

Fig. 1(a) shows the SYM-H index, the solar wind magnetic field and plasma data from WIND during 17–19 April 2002 when a typical magnetic cloud (MC) was detected. The MC arrived at 0000 UT on 18 April (indicated by the vertical line MC_f) and extended to 0600 UT on 19 April (MC_t). The upstream sheath region extended from the arrival of the MC-driven shock (S) at 1101 UT on 17 April to the MC leading edge. The sheath/MC boundary is identified by the decrease in proton temperature below that expected for normal solar wind expansion, as shown by the thick solid trace in the T_p panel (see Richardson and Cane (1995) for details). The magnitude of the magnetic field, plasma bulk velocity, proton temperature, and number density increased significantly across the shock front, which resulted in the enhancements of solar wind dynamic pressure and IEF. At 1107 UT, a storm sudden commencement (SSC) in the SYM-H index induced by this shock was observed. Thus, we can infer that the transit time for the

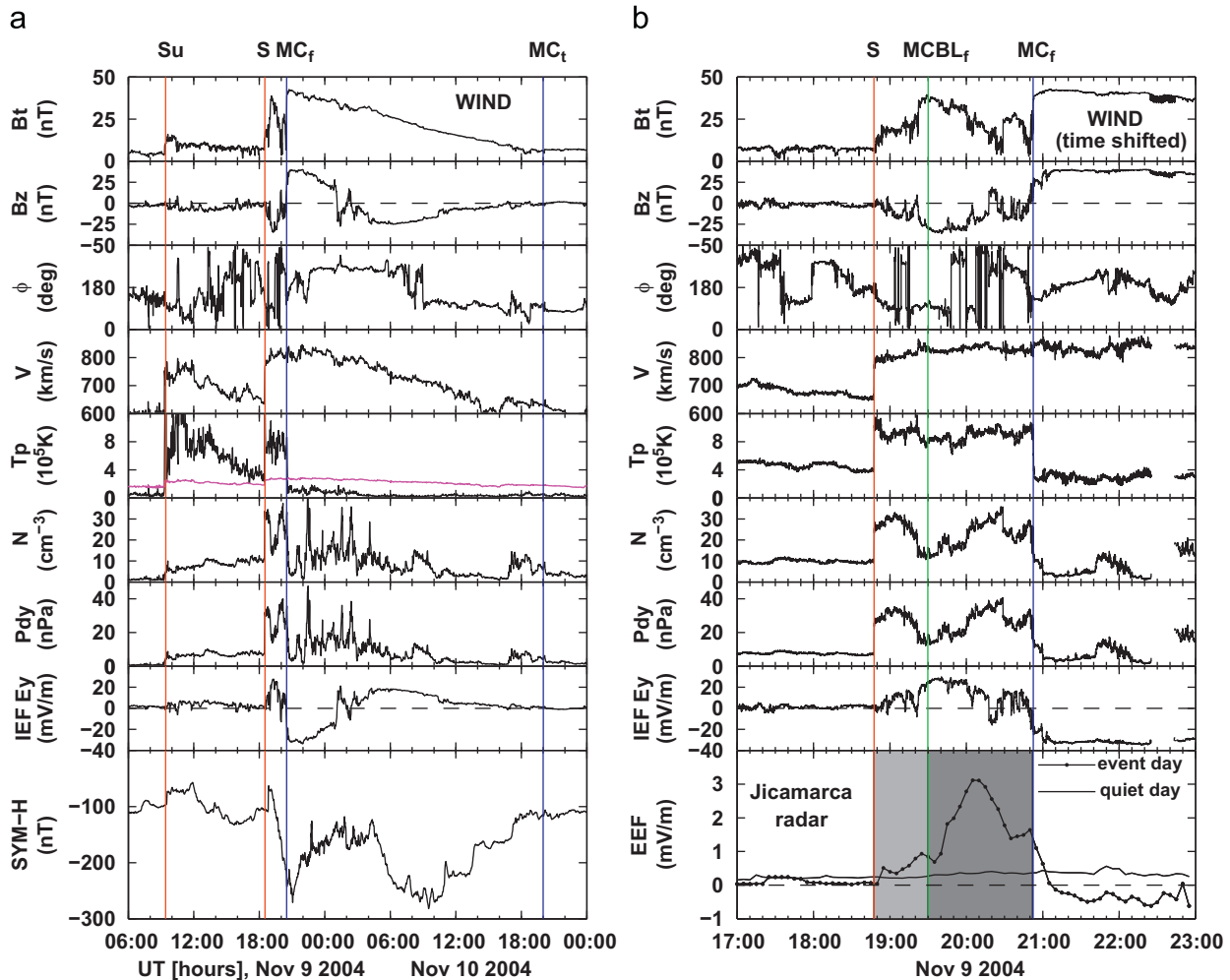


Fig. 2. Solar wind, geomagnetic, and EEF data related to the electric field penetration on 9 November 2004. The EEF data of 11 November 2004 are plotted as a quiet-time reference (thick solid line). The lighter and darker shades correspond to the sheath region and MCBL interval, respectively.

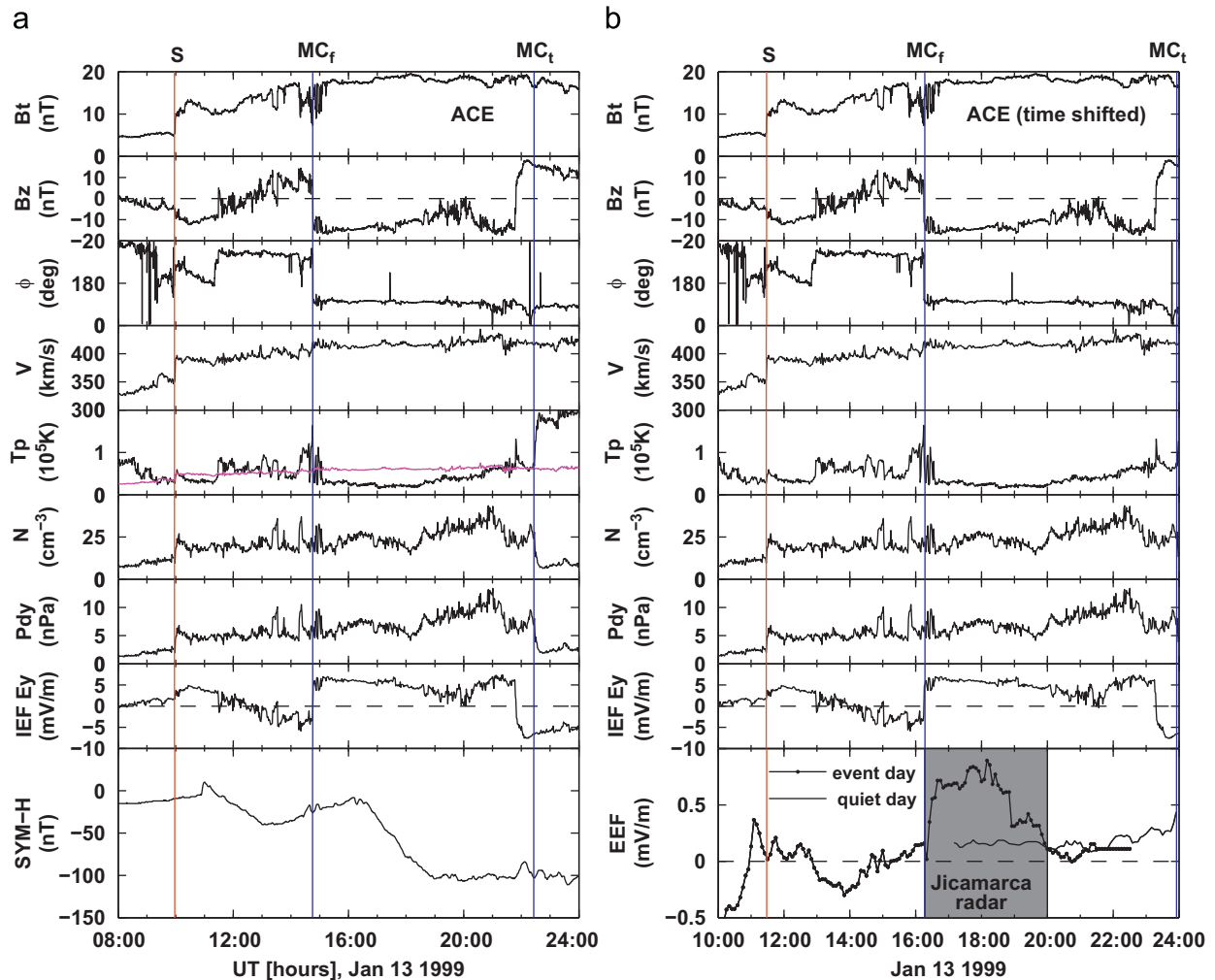


Fig. 3. Solar wind, geomagnetic, and EEF data related to the electric field penetration on 13 January 1999. The EEF data of 12 January 1999 are plotted as a quiet-time reference (thick solid line). Note that the solar wind data are from ACE instead of WIND because of a data gap, but the time-shift is determined according to the WIND data (not shown) as well as the SYM-H index.

shock from the WIND spacecraft to the magnetopause is about 6 min for this case. Fig. 1(b) displays the observations of the equatorial electric field (EEF) for the period 1000–2200 UT on 17 April and the corresponding solar wind fine structures, that have been shifted to their arrival time at the magnetopause according to the transit time described above. Immediately following the shock arrival, the EEF oscillated with the same period as the IMF within the sheath, which was attributed to the penetration of IEF (see Kelley et al. (2003) and Huang et al. (2005)). The shaded interval denotes the occurrence of the penetration electric field associated with the sheath region. Note that, due to the less geoeffectiveness within the trailing edge of the sheath region (from about 2100–2400 UT on 17 April), no obvious penetration electric field was measured for this period.

Fig. 2(a) shows the interplanetary conditions and the SYM-H index during 9–10 November 2004. A MC arrived at 2030 UT on 9 November and extended to 2000 UT on 10 November. The MC-driven shock arrived at 1825 UT on 9 November. In addition, an unrelated shock (S_u) was propagating through the preceding MC at 0925 UT on 9 November; this shock-running-into-preceding-CME scenario is caused by the occurrence of two successive CMEs within a relatively short period (see Zhang et al. (2008) for details). At 1848 UT, a SSC in the SYM-H index associated with this shock was observed. Fig. 2(b) displays the EEF

for the period 1700–2300 UT on 9 November and the corresponding solar wind fine structures with a 23 min time-shift (transit time of the shock). In the bottom panel, the EEF data of 11 November 2004 are plotted as a quiet-time reference (thick solid line), and the purpose is to compare the change of the EEF in response to IMF reorientations with the values over a relatively quiet day. A typical magnetic cloud boundary layer (MCBL) is observed between the sheath and the MC body during the interval of 1930–2053 UT ($MCBL_f-MC_f$). Generally, the MCBLs are characterized by the obvious magnetic signatures including the magnetic decrease inside the boundary layer, the magnetic field azimuthal angle and the latitudinal angle change near the center of MCBLs, as well as the corresponding plasma features: relatively high proton temperature, high plasma β , high proton density, and high dynamic pressure (Wei et al., 2003a; 2003b; 2006; Zuo et al., 2007). The lighter shading between 1848 and 1930 UT corresponds to the interval of the sheath region, during which the eastward EEF was enhanced gradually to about 1 mV/m. The MCBL (indicated by the darker shading) clearly stood out as being important drivers of the pronounced EEF increase during the interval 1930–2053 UT, which reached its maximum at about 2000 UT; it is the largest daytime value (over 3 mV/m) ever measured by the radar (Fejer et al., 2007; Kelley et al., 2009). During the entire interval of the sheath region and MCBL, the

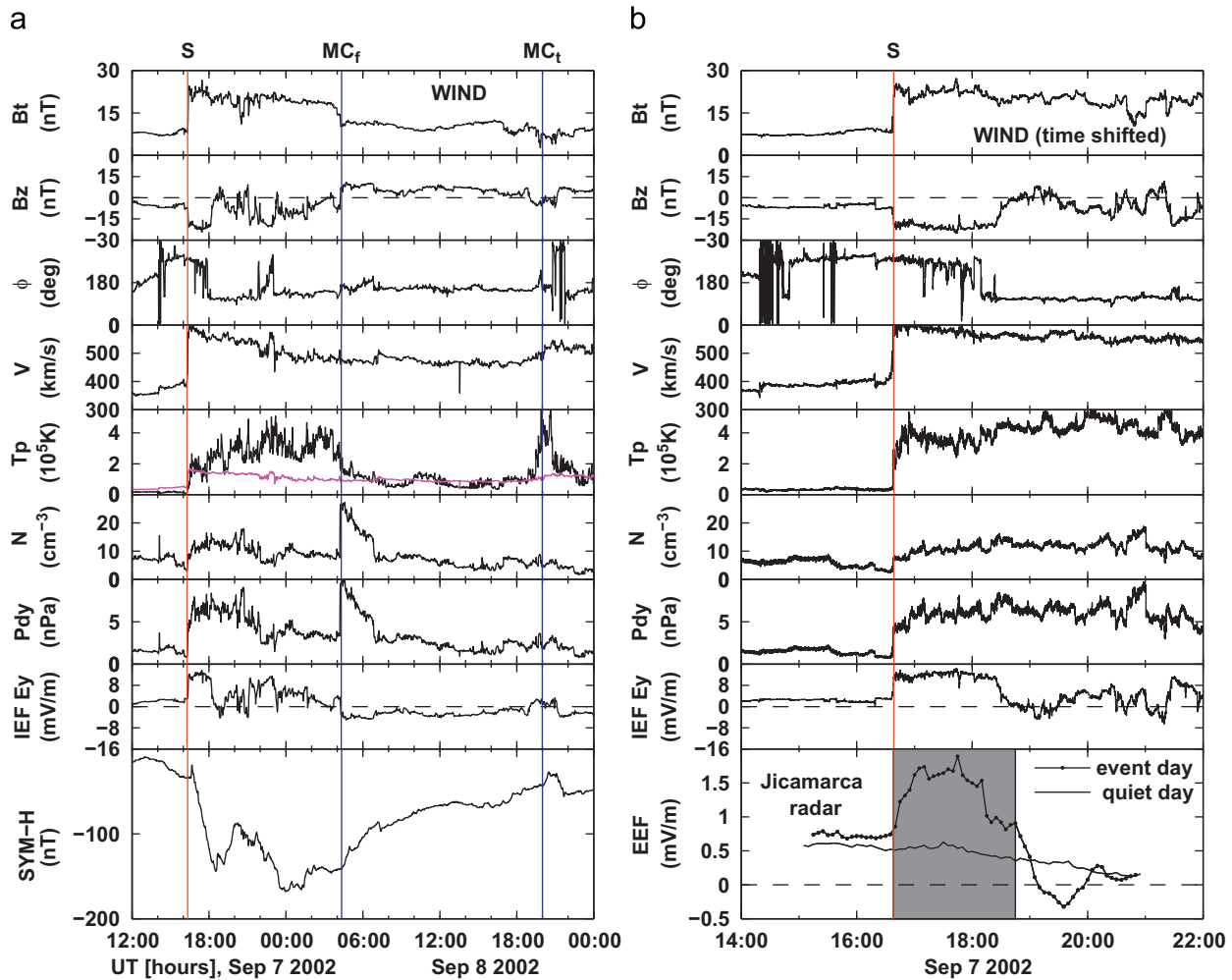


Fig. 4. Solar wind, geomagnetic, and EEF data related to the electric field penetration on 7 September 2002. The EEF data of 6 September 2002 are plotted as a quiet-time reference (thick solid line). Note that the EEF data are inferred from the Doppler shifts of 150-km echoes.

shape of the enhanced eastward EEF is very similar to the positive enhancement of the IEF, indicating that the IEF penetrated to the equatorial ionosphere. Therefore, the *sheath region together with MCBL* caused this penetration event.

Fig. 3(a) shows the magnetic field and plasma data detected by ACE instead of WIND because of a data gap, as well as the SYM-H index on 13 January 1999. A MC arrived at 1446 UT and extended to 2225 UT. The upstream sheath region extended from the arrival of the MC-driven shock at 0958 UT to the MC leading edge. At 1056 UT, a SSC in the SYM-H index associated with this shock was observed. Fig. 3(b) displays the EEF for the period 1000–2400 UT and the corresponding solar wind fine structures with 89 min time-shift. In the bottom panel, the EEF data of 12 January 1999 are plotted as a quiet-time reference (thick solid line). It is important to note that this time-shift is implemented according to the WIND observation (not shown) as well as the SSC, considering a relatively great propagation distance of solar wind from ACE to the magnetopause. Shortly after the MC leading edge arrival, the EEF presented eastward surges of order 0.8–0.9 mV/m. Later, it decreased gradually and became close to the quiet-day value at about 2000 UT. These observed features suggest that the penetration electric field occurred during the period from about 1620 UT to 2000 UT (indicated by the gray shading) and was caused by the MC body.

Fig. 4(a) shows the interplanetary situation and the SYM-H index during 7–8 September 2002. A shock observed at 1622 UT

on 7 September was propagating through a preceding and unrelated MC at the time of observation, which has been identified by Zhang et al., (2008). The magnetic field in the preceding MC ahead of the shock was southward. Compression by the shock then enhanced the negative Bz component by a factor of about two, which resulted in the enhancement of eastward EEF (described below). At 1637 UT, a SSC in the SYM-H index associated with this shock was observed. Fig. 4(b) displays the EEF determined from the Doppler shifts of 150-km echoes for the period 1400–2400 UT on 7 September 2002, and the corresponding solar wind fine structures with 15 min time-shift (transit time of the shock). In the bottom panel, the EEF data of 6 September 2002 are plotted as a quiet-time reference (thick solid line). The shaded interval denotes the occurrence of the penetration electric field (cf. Huang et al., 2005) and corresponds to the negative Bz component enhancement within the sheath region, during which the EEF increased rapidly from 0.8 mV/m to about 1.6 mV/m. Thus this electric field penetration event is associated with a *shock-running into a preceding MC*.

3. Summary and discussion

We have discussed the penetration effects of common MC structures like sheath region, both sheath and MCBL, MC body, and shock-running into a preceding MC on the equatorial

ionosphere during intense geomagnetic storms. In four cases, after elimination of the propagation delay, the EEF was changed immediately following the arrival of solar wind disturbance. This is consistent with the suggestions by Manoj et al. (2008) that the time delay between IEF and EEF is less than 5 min at all periods. Moreover, the duration of EEF corresponded well with that of the corresponding MC structure interval.

Low latitude ionospheric electric field perturbations during geomagnetic active times are due mostly to the combined effects of relatively short-lived prompt penetration and longer lasting ionospheric disturbance dynamo electric fields (Fejer et al., 2007). In the cases of Figs. 2–4, the daytime EEF enhancements detected by the Jicamarca radar are caused by IEF penetration because the EEF is clearly correlated with the IEF and because no dynamo electric field at low latitudes can be generated within the first 2–3 h of a magnetic storm. During magnetic storms, energy input from the magnetosphere into the ionospheric auroral zone will launch atmospheric disturbances. In general, even large-scale atmospheric disturbances during intense storms will take 2–3 h travel to low latitudes (Fuller-Rowell et al., 1994), so dynamo electric field at low latitudes can be generated 2–3 h after SSC. However, the enhancement of the EEF in the cases of Figs. 2–4 occurred almost immediately after SSC; this enhancement cannot be attributed to dynamo process because atmospheric disturbances cannot travel to the equatorial ionosphere within 2 h. In the case of Fig. 1, the first 2–3 h EEF fluctuations are due to IEF penetration, while the latter fluctuations may be due to the compounded effects of IEF penetration and dynamo electric field.

The magnetic fields have a significantly different behavior during the MC structures presented in this paper. A MC is a flux rope structure with smoothly rotating magnetic fields (Klein and Burlaga, 1982). Southward fields may be found either in the leading or trailing part of MCs, or close to their centers, depending on the orientation of the MC axis (Lepping et al., 1990; Wu and Lepping, 2002). Within the sheath region, the magnetic field direction can change several times between south and north. The magnetic field Z component (B_z) has more turbulent structure inside boundary layers than inside sheath regions and MC (Zuo et al., 2007). The different behavior of the magnetic fields in MC structures may cause different penetration characters (e.g. the duration and strength). For instance, in the case on 13 January 1999, the EEF enhancements was caused by the IMF southward structure in the leading part of the MC, while in the case on 17 April 2002, the EEF oscillated with the same period of the IMF within the sheath.

Our observations clearly indicate that the EEF is not proportional to the IEF except the penetration event on 17 April 2002, for which the EEF showed a good correlation with the IEF ($r \sim 0.7$) (Kelley et al., 2003). The ratio of EEF and IEF varied between about 0.25 and 0.59 during penetration interval on 9 November 2004, while between 0.02 and 0.15 for the case on 13 January 1999 and between 0.08 and 0.15 for the case on 7 September 2002. In fact, prior experimental and model studies suggested that the magnitude of the prompt penetration electric fields is local time dependent and that they have strong dependence on magnetospheric (e.g., ring current ion pressure) and ionospheric parameters (e.g., conductance) (Fejer et al., 2007 and references therein).

In short, we discussed the penetration effects of common MC structures like sheath region, both sheath and MCBL, MC body, and shock-running into a preceding MC on the equatorial ionosphere during intense geomagnetic storms. After elimination of the propagation delay, the equatorial electric field (EEF) was changed immediately following the arrival of solar wind disturbance. Moreover, the duration of EEF corresponded well with

that of the corresponding MC structure interval. We believe that the knowledge of the interplanetary driver of the penetration electric field could help: (1) gain new physical insight into penetration processes (such as the driving mechanisms, the penetration duration and strength), and (2) explore the effect of the penetration electric field on the ionospheric plasma.

Acknowledgements

Jianpeng Guo thanks Dr. Jiuhou Lei for valuable suggestions. The Jicamarca Radio Observatory is a facility of the Instituto Geofísico del Perú operated with support from the NSF Cooperative Agreement ATM-0432565 through Cornell University. We acknowledge the CDAWeb for access to the Wind and ACE data. The SYM-H data is provided by the World Data Center for Geomagnetism at Kyoto University. This work is jointly supported by the National Natural Science Foundation of China (40921063, 40890162, 0674084 and 40804046), 973 Program under grant 2006CB806304, the Specialized Research Fund for State Key Laboratories, and the National Science Foundation for Post-doctoral Scientists of China (20090450589).

References

- Burlaga, L.F., Sittler, E., Mariani, F., Schwenn, R., 1981. Magnetic loop behind and interplanetary shock: voyager, helios, and IMP 8 observations. *Journal of Geophysical Research* 86, 6673–6684.
- Burlaga, L.F., Plunkett, S.P., Cyr St., O.C., 2002. Successive CMEs and complex ejecta. *Journal of Geophysical Research* 107 (A10), 1266.
- Cane, H.V., Richardson, I.G., 2003. Interplanetary coronal mass ejections in the near-Earth solar wind during 1996–2002. *Journal of Geophysical Research* 108 (A4), 1156.
- Chau, J.L., Woodman, R.F., 2004. Daytime vertical and zonal velocities from 150-km echoes: their relevance to F region dynamics. *Geophysical Research Letters* 31, L17801.
- Dungey, J.W., 1961. Interplanetary magnetic field and the auroral zones. *Physical Review Letters* 6, 47.
- Earle, G.D., Kelley, M.C., 1987. Spectral studies of the sources of ionospheric electric fields. *Journal of Geophysical Research* 92 (A1), 213–224.
- Fejer, B.G., Spiro, R.W., Wold, R.A., Foster, J.C., 1990. Latitudinal variations of penetration electric fields during magnetically disturbed periods: 1986 SUNDIAL observations and model results. *Annales Geophysicae* 8, 441.
- Fejer, B.G., Jensen, J.W., Kikuchi, T., Abdu, M.A., Chau, J.L., 2007. Equatorial ionospheric electric fields during the November 2004 magnetic storm. *Journal of Geophysical Research* 112, A10304.
- Fuller-Rowell, T.J., Codrescu, M.V., Moffett, R.J., Quegan, S., 1994. Response of the thermosphere and ionosphere to geomagnetic storms. *Journal of Geophysical Research* 99, 3893.
- Gopalswamy, N., Yashiro, S., Kaiser, M.L., Howard, R.A., Bougeret, J.L., 2001. Radio signatures of coronal mass ejection interaction: coronal mass ejection cannibalism? *Astrophysical Journal* 548, L91–L94.
- Huang, C.-S., Foster, J.C., Kelley, M.C., 2005. Long-duration penetration of the interplanetary electric field to the low-latitude ionosphere during the main phase of magnetic storms. *Journal of Geophysical Research* 110, A11309.
- Huang, C.-S., Sazykin, S., Chau, J.L., Maruyama, N., Kelley, M.C., 2007. Penetration electric fields: efficiency and characteristic time scale. *Journal of Atmospheric and Solar Terrestrial Physics* 69 (10–11), 1135–1146.
- Huttunen, K.E.J., Koskinen, H.E.J., 2004. Importance of postshock streams and sheath region as drivers of intense magnetospheric storms and high-latitude activity. *Annales Geophysicae* 22, 1729–1738.
- Huttunen, K.E.J., Kilpua, S.P., Pulkkinen, A., Viljanen, A., Tanskanen, E., 2008. Solar wind drivers of large geomagnetically induced currents during the solar cycle 23. *Space Weather* 6, S10002.
- Kelley, M.C., Fejer, B.G., Gonzales, C.A., 1979. An explanation for anomalous equatorial ionospheric electric field associated with a northward turning of the interplanetary magnetic field. *Geophysical Research Letters* 6 (4), 301.
- Kelley, M.C., Makela, J.J., Chau, J.L., Nicolls, M.J., 2003. Penetration of the solar wind electric field into the magnetosphere/ionosphere system. *Geophysical Research Letters* 30 (4), 1158.
- Kelley, M.C., Ilma, R.R., Nicolls, M., Erickson, P., Goncharenko, L., Chau, J.L., Aponte, N., Kozyra, J.U., 2009. Spectacular low and mid-latitude electrical fields and neutral winds during a superstorm. *Journal of Atmospheric and Solar Terrestrial Physics*.
- Kikuchi, T., Araki, T., 1979. Horizontal transmission of the polar electric field to the equator. *Journal of Atmospheric and Solar Terrestrial Physics* 41, 917.
- Klein, L.W., Burlaga, L.F., 1982. Interplanetary magnetic clouds at 1 AU. *Journal of Geophysical Research* 87, 613–624.

- Lepping, R.P., Jones, J.A., Burlaga, L.F., 1990. Magnetic field structure of interplanetary magnetic clouds at 1 AU. *Journal of Geophysical Research* 95, 11,957–11,965.
- Lepri, S.T., Zurbuchen, T.H., Fisk, L.A., Richardson, I.G., Cane, H.V., Gloeckler, G., 2001. Iron charge distribution as an identifier of interplanetary coronal mass ejections. *Journal of Geophysical Research* 106 (A12), 29,231–29,238.
- Manoj, C., Maus, S., Lühr, H., Alken, P., 2008. Penetration characteristics of the interplanetary electric field to the daytime equatorial ionosphere. *Journal of Geophysical Research* 113, A12310.
- Nicolls, M.J., Kelley, M.C., Chau, J.L., Veliz, O., Anderson, D., Anghel, A., 2007. The spectral properties of low latitude daytime electric fields inferred from magnetometer observations. *Journal of Atmospheric and Solar Terrestrial Physics* 69 (10–11), 1160–1173.
- Nopper, R.W., Carovillano, R.L., 1978. Polar-equatorial coupling during magnetically active periods. *Geophysical Research Letters* 5 (8), 699.
- Richardson, I.G., Cane, H.V., 1995. Regions of abnormally low proton temperature in the solar wind (1965–1991) and their association with ejecta. *Journal of Geophysical Research* 100 (A12), 23,397–23,412.
- Richardson, I.G., Cane, H.V., 2004. The fraction of interplanetary coronal mass ejections that are magnetic clouds: evidence for a solar cycle variation. *Geophysical Research Letters* 31, L18804.
- Senior, C., Blanc, M., 1984. On the control of magnetospheric convection by the spatial distribution of ionospheric conductivity. *Journal of Geophysical Research* 89, 261–284.
- Tsurutani, B.T., Gonzalez, W.D., Tang, F., Akasofu, S.I., Smith, E.J., 1988. Origin of interplanetary southward magnetic fields responsible for major magnetic storms near solar maximum (1978–1979). *Journal of Geophysical Research* 93, 8519–8531.
- Tsurutani, B.T., et al., 2008. Prompt penetration electric fields (PPEFs) and their ionospheric effects during the great magnetic storm of 30–31 October 2003. *Journal of Geophysical Research* 113, A05311.
- Wei, F., Liu, R., Fan, Q., Feng, X., 2003a. Identification of the magnetic cloud boundary layers. *Journal of Geophysical Research* 108 (A6), 1263.
- Wei, F., Liu, R., Feng, X., Zhong, D., Yang, F., 2003b. Magnetic structures inside boundary layers of magnetic clouds. *Geophysical Research Letters* 30 (24), 2283.
- Wei, F., Feng, X., Yang, F., Zhong, D., 2006. A new non-pressure-balanced structure in interplanetary space: boundary layers of magnetic clouds. *Journal of Geophysical Research* 111, A03102.
- Wei, Y., Hong, M., Wan, W., Du, A., Lei, J., Zhao, B., Wang, W., Ren, Z., Yue, X., 2008. Unusually long lasting multiple penetration of interplanetary electric field to equatorial ionosphere under oscillating IMF Bz. *Geophysical Research Letters* 35, L02102.
- Wolf, R.A., Spiro, R.W., Sazykin, S., Toffoletto, F.R., 2007. How the Earth's inner magnetosphere works: an evolving picture. *Journal of Atmospheric and Solar Terrestrial Physics* 69 (3), 288–302.
- Wu, C., Lepping, R.P., 2002. Effects of magnetic clouds on the occurrence of geomagnetic storms: the first 4 years of wind. *Journal of Geophysical Research* 107 (A10), 1314.
- Zhang, J., Richardson, I.G., Webb, D.F., 2008. Interplanetary origin of multiple-dip geomagnetic storms. *Journal of Geophysical Research* 113, A00A12.
- Zuo, P.B., Wei, F.S., Feng, X.S., Yang, F., 2007. The relationship between the magnetic cloud boundary layer and the substorm expansion phase. *Solar Physics* 242, 167–185.
- Zurbuchen, T.H., Richardson, I.G., 2006. In-situ solar wind and magnetic field signatures of interplanetary coronal mass ejections. *Space Science Review* 123, 31–43.